A&A 521, L18 (2010)
DOI: 10.1051/0004-6361/201015091

Astronomy & Astrophysics
Special feature

Herschel/HIFI: first science highlights

Letter to the Editor

[CII] observations of H_2 molecular layers in transition clouds⋆

T. Velusamy, W. D. Langer, J. L. Pineda, P. F. Goldsmith, D. Li, and H. W. Yorke

Jet Propulsion Laboratory, California Institute of Technology, 4800 Oak Grove Drive, Pasadena, CA 91109-8099, USA
e-mail: velusamy@jpl.nasa.gov

Received 31 May 2010 / Accepted 15 July 2010

ABSTRACT

We present the first results on the diffuse transition clouds observed in [CII] line emission at 158 μm (1.9 THz) towards Galactic longitudes near 340° (5 LOSs) & 20° (11 LOSs) as part of the HIFI tests and GOT C+ survey. Out of the total 146 [CII] velocity components detected by profile fitting we identify 53 as diffuse molecular clouds with associated ^{12}CO emission but without ^{13}CO emission and characterized by $A_V < 5$ mag. We estimate the fraction of the [CII] emission in the diffuse HI layer in each cloud and then determine the [CII] emitted from the molecular layers in the cloud. We show that the excess [CII] intensities detected in a few clouds is indicative of a thick H_2 layer around the CO core. The wide range of clouds in our sample with thin to thick H_2 layers suggests that these are at various evolutionary states characterized by the formation of H_2 and CO layers from HI and C^+, respectively. In about 30% of the clouds the H_2 column densities ("dark gas") traced by the [CII] is 50% or more than that traced by ^{12}CO emission. On the average ~25% of the total H_2 in these clouds is in an H_2 layer which is not traced by CO. We use the HI, [CII], and ^{12}CO intensities in each cloud along with simple chemical models to obtain constraints on the FUV fields and cosmic ray ionization rates.

Key words. ISM: structure – ISM: molecules — ISM: atoms – submillimeter: ISM

1. Introduction

The *Herschel* key program GOT C+ (Galactic Observations of Terahertz C^+) is designed to study the diffuse interstellar medium (ISM) by observing with the HIFI instrument the [CII] $^2P_{3/2} \rightarrow {}^2P_{1/2}$ fine structure line emission and absorption at 1.9 THz (158 μm) over a volume weighted sampling of 500 lines of sight (LOSs) throughout the Galactic disk. The GOT C+ project is described by Langer et al. (2010a) and the use of [CII] emission to detect diffuse warm "dark gas" (H_2 molecular gas not seen by CO observations) by Langer et al. (2010b). C^+ is a major ISM coolant, and its 158 μm line is an important tracer of the properties of the diffuse atomic and diffuse molecular gas clouds. The [CII] line thus enables us to trace an important but to date poorly-studied stage in cloud evolution - the transition clouds going from atomic to molecular: HI to H_2 and C^+ to CI and CO (Snow & McCall 2006). These clouds have a large molecular hydrogen fraction in which carbon exists primarily as C^+ rather than as CO (Tielens & Hollenbach 1985; van Dishoeck & Black 1988). Transition clouds are difficult to study using the standard tracers (HI or CO) but [CII] can trace this gas.

There is growing evidence that a substantial amount of interstellar gas exists as molecular H_2, not traced by CO, for example: from gamma-ray data from EGRET (e.g. Grenier et al. (2005)) and Fermi-LAT (e.g. Abdo et al. 2010); and, the infrared continuum in diffuse clouds (Reach et al. 1994). Goldsmith et al. (2010) detected warm H_2 in emission beyond the CO extent of Taurus. Wolfire et al. (2010) have modeled the molecular cloud surfaces to estimate the amount of "dark gas" in the form of molecular H_2 in the H_2/C^+ layers and find it contributes about 30% of the total mass in clouds with total $A_V \sim 8$ mag. Here, we present direct observational evidence for the H_2/C^+ layer in a number of transition clouds through the detection of an excess [CII] line emission in them. We use a sample of 53 transition clouds characterized by $A_V < 5$ mag. and the presence of both HI and ^{12}CO emissions but no ^{13}CO. We analyze the observed [CII] intensities combined with HI and CO data to obtain an inventory of the total molecular H_2 in different layers in transition clouds and then constrain the physical conditions by applying simple models for CO formation and photodissociation.

2. Observations and data analysis

The observations reported here were made as part of the HIFI performance verification and priority science phases. We observed the [CII] line at 1900.5469 GHz towards 16 LOSs in the galactic plane with the HIFI (de Graauw et al. 2010) instrument on the *Herschel* Space Observatory (Pilbratt et al. 2010). The [CII] spectra were obtained using the wide band spectrometer (with 0.22 km s^{-1} velocity resolution, over 350 km s^{-1} range) at band 7b and using integration of 800 s to 1800 s (with rms of 0.1 K to 0.2 K on data smoothed to 1 km s^{-1}). For each target we used the load chop (HPoint) with a sky reference offset by 2° in latitude. The data were processed in HIPE version 3.0 using the standard pipeline for HIFI. Using a fringe fitting tool within HIPE we were able to mitigate the standing waves in band 7b (Higgins & Kooi 2009) to sufficiently low levels to provide good baselines in the [CII] spectra (Boogert, priv. comm.). The data presented here are in the Galactic plane at l = 337.8°, 343.04°, 343.91°, 344.78°, 345.65°, 18.3°, 22.6°, 23.5°& 24.3°; out of the plane at $b = 0.5°$ for $l = 24.3°$and $b = 1°$ at $l = 22.6°$& 24.3°; at $b = -0.5°$& -1°at $l = 18.3°$ & 23.5°. Table 1 summarizes all the observational data used in our analysis.

An example of the [CII] spectrum is shown in the top panel in Fig. 1. The [CII] intensities were corrected for main beam efficiency (~0.63). For comparison the HI and the CO spectra are

⋆ *Herschel* is an ESA space observatory with science instruments provided by European-led Principal Investigator consortia and with important participation from NASA.

Table 1. Observational data.

Line	Survey facility	Beam	Velocity chan. [km s^{-1}]	Sensitivity chan. [K km s^{-1}]	Ref.
[CII] 1.9 THz	GOT C+ *Herschel* HIFI	12″	1.0	0.1–0.2	1,2
HI	SGPS/ATCA	132″	0.84	1.6	3
	VGPS/VLA	60″	0.84	2.0	4
^{12}CO (1-0)	ATNF	33″	0.8	0.6	5
^{13}CO (1-0)	Mopra		0.8	0.1	
C^{18}O (1-0)	22-m		1.6	0.1	

Notes. (1) This paper; (2) Langer et al. (2010a); (3) McClure-Griffiths et al. (2005); (4) Stil et al. (2006); (5) Pineda et al. (2010).

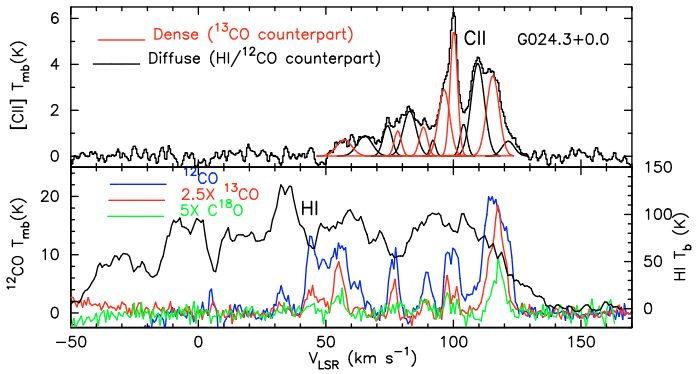

Fig. 1. An example of [CII] spectrum for l = 24.3°, b = 0.0° and Gaussian fits marked in red and black (*top panel*) and ancillary data (*lower panel*).

shown in the lower panel. The [CII] spectra show many velocity resolved features. All [CII] emission features show an overall correlation with the HI, though not all HI features show corresponding [CII] emission. Many [CII] features are also correlated with CO features. To separate the individual velocity components we used multiple Gaussian fitting. In the case of complex (overlapping) velocity features we used both [CII] and HI profiles together to identify the individual components. We identified a total of 146 velocity components in all the LOSs. As seen in Fig. 1 as well as in the examples shown in Langer et al. (2010b) & Pineda et al. (2010) in each spectrum we detect many velocity components. However, their identity as clouds is somewhat uncertain as the decomposition itself is not very unique and may not be reliable (e.g. Falgarone et al. 1994). Though we use the HI profile as an independent check on the features, the beam sizes (Table 1) are not modeled into the decomposition. For simplicity, here we refer to them as clouds, but in reality some of them may be for example, isolated turbulent clumps, transient fluctuations of larger structures, or superposition of extremely narrow velocity components. In view of the uncertainties, for all our quantitative analysis we do not use all of the Gaussian fit parameters. Instead we use the fitted $V_{\rm LSR}$ to locate a parcel of the gas at a certain velocity and width. The I(CII), I(HI), I(^{12}CO) intensities for each cloud were then obtained, in a consistent manner, by integrating the intensities ($T_{\rm mb}$) over the velocity width (ΔV) centered at the respective $V_{\rm LSR}$ (except in a few cases which are confused by the adjacent component).

We identified 58 [CII] components as dense molecular clouds traced by their ^{13}CO emission (e.g. the red Gaussian fits in Fig. 1) and these are discussed in a separate paper by Pineda et al. (2010). We regard the remaining 88 components without ^{13}CO counterparts (e.g. the black Gaussian fits in Fig. 1) as diffuse clouds, envelopes or transition clouds. We examined

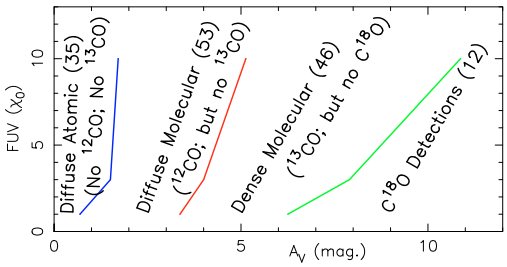

Fig. 2. The [CII] cloud samples identified as a function $A_{\rm V}$ and FUV field. The lines mark the boundaries needed to form a detection threshold of CO species. The number of clouds in each category is indicated.

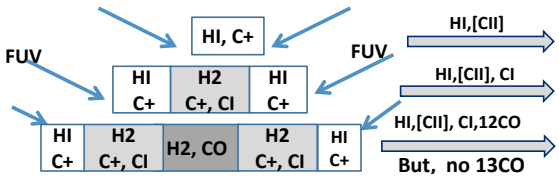

Fig. 3. Schematic of the diffuse clouds observed in our sample.

these 88 diffuse [CII] clouds by correlating them with the ^{12}CO spectra. We found that 53 components have associated ^{12}CO emission while the remaining 35 have no ^{12}CO counterparts. These 35 clouds are labeled diffuse atomic clouds of which 29 are discussed by Langer et al. (2010b). To place our [CII] cloud samples in the context of the general interstellar clouds, in Fig. 2 we identify them in an $A_{\rm V}$ - FUV parameter space. We use our 3-σ detection limits (Table 1) for [CII], ^{12}CO, ^{13}CO, and C^{18}O to estimate the corresponding thresholds of $A_{\rm V}$ and FUV based on the calculations by Visser et al. (2009). The Visser et al. calculations use $T_{\rm gas}$ = 100 K, and $n_{\rm H}$ = 300 cm^{-3} similar to what we use below in our analysis. Here we present results on 50 transition clouds excluding 3 for data quality and other issues.

3. Results and discussion

3.1. [CII] sample of transition clouds

In Fig. 2 we find that our [CII] sample of transition clouds are diffuse having $A_{\rm V} \leq$ 3–4 mag. for reasonable interstellar FUV, in the range of 1–10$\chi_{\rm D}$ (the average FUV intensity $\chi_{\rm D} \sim 2.2 \times 10^{-4}$ erg cm^{-2} s^{-1}sr^{-1} Draine 1978). In Fig. 3 we show a schematic of the diffuse cloud layers. In the dense cores with ^{13}CO emission, the conversion of C$^+$ to CO is more complete while it is partial in these diffuse transition clouds due to lack of sufficient self-shielding. All clouds contain some quantity of HI. As seen in Fig. 3, the observed [CII] emission originates from the purely atomic HI layer along with a contribution from the H$_2$/C$^+$ layer, while the ^{12}CO emission originates in the H$_2$/CO core. Thus estimates of H$_2$ column densities using ^{12}CO intensity alone entirely misses the H$_2$ in the H$_2$/C$^+$ ("dark gas") layer. Therefore, a complete inventory of molecular H$_2$ in the cloud requires both the [CII] and ^{12}CO intensities.

3.2. [CII] in the HI/C$^+$ layer

In Fig. 4a we plot the [CII] intensities against the HI intensities for all 50 transition clouds. The error bars in Figs. 4a,b represent the 1-σ uncertainties in the respective measured intensities. In spite of the large scatter we note a lower bound to I(CII) that increases gradually with I(HI) which is consistent with the [CII] emission expected from a HI/C$^+$ layer (Fig. 3). For quantitative

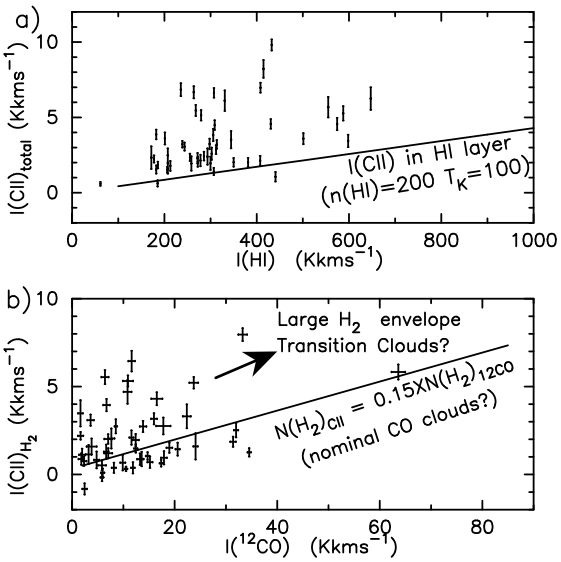

Fig. 4. a) The observed [CII] versus HI intensities: The line is a fit for $I(\mathrm{CII})_{\mathrm{HI}}$ in "nominal" HI clouds (see text). The intensities above this line represent that arising from C^+ in the H_2 layer surrounding the ^{12}CO emitting core. **b)** $I(\mathrm{CII})_{\mathrm{H_2}}$, the excess obtained as $I(\mathrm{CII}) - I(\mathrm{CII})_{\mathrm{HI}}$ is plotted against $I(^{12}\mathrm{CO})$. The line is a fit to [CII] intensities from "nominal" clouds containing about 15% of the total H_2 in the H_2/C^+ layer (see text). Clouds with larger H_2 envelopes lie above this line.

analysis of [CII] emission from the HI/C^+ layer we use the following steps (see Langer et al. 2010b):

i) The observed I(CII) is regarded as the total $I(\mathrm{CII})_{\mathrm{total}} = I(\mathrm{CII})_{\mathrm{HI}} + I(\mathrm{CII})_{\mathrm{H_2}}$, where $I(\mathrm{CII})_{\mathrm{HI}}$ and $I(\mathrm{CII})_{\mathrm{H_2}}$ are the emissions originating from the HI/C^+ and H_2/C^+ layers respectively with no [CII] emission from the ^{12}CO emitting core (Fig. 3).
ii) Use the HI intensity, I(HI) to estimate the HI column density, $N(\mathrm{HI}) = 1.82 \times 10^{18} I(\mathrm{HI})$ cm^{-2}.
iii) Use N(HI) to estimate the C^+ column density in the HI/C^+ layer, $N(\mathrm{C^+})_{\mathrm{HI}} \sim X(\mathrm{C^+})N(\mathrm{HI})$, where $X(\mathrm{C^+}) = n(\mathrm{C^+})/n(\mathrm{HI})$ is assumed to be 1.5×10^{-4}.
iv) Using the $N(\mathrm{C^+})_{\mathrm{HI}}$ above we calculate $I(\mathrm{CII})_{\mathrm{HI}} \sim f((n(\mathrm{HI}), T_K) \times N(\mathrm{C^+})_{\mathrm{HI}}$, where the function f accounts for the excitation conditions for density n(HI) and temperature T_K (see Langer et al. 2010b). Then we can express it in terms I(HI), as $I(\mathrm{CII})_{\mathrm{HI}} \propto f(n(\mathrm{HI}), T_K) I(\mathrm{HI})$.

We find that on average the form of I(CII) versus I(HI) can be fitted by a straight line obtained for density n(HI) ~ 200 cm^{-3} at temperature $T_K \sim 100$ K as shown in Fig. 4a. In more massive clouds with HI intensities greater than 1000 K km s^{-1} Wolfire et al. (2010) estimate n(HI) ~50–150 cm^{-3} and $T_K \sim$ 70–80 K. However, all our [CII] clouds are less massive with HI intensities <600 K km s^{-1}. In the present analysis we assume n(HI) ~200 cm^{-3} and $T_K \sim 100$ K which seem to describe best the contribution to the [CII] intensity from the HI/C^+ layer.

3.3. [CII] in the H_2/C^+ layer

Having estimated $I(\mathrm{CII})_{\mathrm{HI}}$ arising from the HI/C^+ layer we can now calculate the [CII] excess arising from the H_2/C^+ layer as $I(\mathrm{CII})_{\mathrm{H_2}} = I(\mathrm{CII})_{\mathrm{total}} - I(\mathrm{CII})_{\mathrm{HI}}$. In Fig. 4b we show this excess plotted against $I(^{12}\mathrm{CO})$. Since all the carbon in the ^{12}CO emitting region is converted to CO we do not expect to see any correlation. However, in spite of the large scatter we do note a lower bound to the excess $I(\mathrm{CII})_{\mathrm{H_2}}$ that increases gradually with

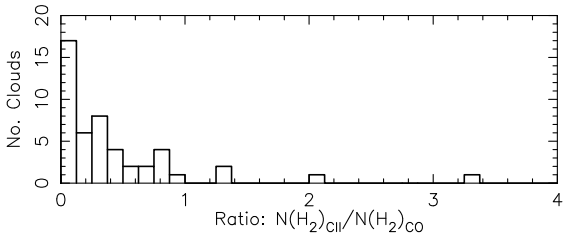

Fig. 5. Number of transition clouds as a function of the ratio of H_2 column densities $N(H_2)$ traced by emissions in [CII] to that in ^{12}CO.

$I(^{12}\mathrm{CO})$ as seen by the straight line fit in Fig. 4b. This suggests the presence of a C^+ layer surrounding the ^{12}CO emitting core as shown in the schematic in Fig. 3. The straight line in Fig. 4b is an approximate fit to the lower bound to the [CII] intensities as a function of $I(^{12}\mathrm{CO})$ and it corresponds roughly to [CII] intensities for clouds with a H_2/C^+ layer containing a H_2 column density ~15% of the H_2 in the CO core; that is, $N(\mathrm{H_2})_{\mathrm{CII}} = 0.15 \times N(\mathrm{H_2})_{^{12}\mathrm{CO}}$ (see below). Therefore this line may be regarded as representing the "nominal" diffuse CO clouds which contain a small H_2 envelope around the CO core. However, the clouds with large [CII] excess well above this line could represent a sample of clouds in transition with larger H_2 envelopes and relatively smaller CO cores. We this excess $I(\mathrm{CII})_{\mathrm{H_2}}$ and the observed $I(^{12}\mathrm{CO})$ to estimate the H_2 column densities in the H_2/C^+ and ^{12}CO layers respectively. For ^{12}CO we use the phenomenological relationship (cf. Dame et al. 2001):

$$N(\mathrm{H_2})_{^{12}\mathrm{CO}} \sim 1.8 \times 10^{20} I(^{12}\mathrm{CO})\ \mathrm{cm}^{-2}.$$

In the H_2/C^+ layers the C^+ excitation is by H_2 molecules and we can use the [CII] excess shown in Fig. 4b to derive the $N(\mathrm{H_2})_{\mathrm{CII}}$ column density as follows:

i) Use the $I(\mathrm{CII})_{\mathrm{H_2}}$ to calculate the C^+ column density, $N(\mathrm{C^+})_{\mathrm{H_2}}$ in the H_2/C^+ layer, as a function of density $n(H_2)$ and temperature (T_K). Here we assume a higher density of $n(H_2) \sim 300$ cm^{-3} than in the HI layer and a temperature $T_K \sim 100$ K.
ii) Use this $N(C^+)$ column density to estimate $N(H_2) = N(\mathrm{C^+})/2\mathrm{X}(\mathrm{C^+})$, where $X(\mathrm{C^+}) = 1.5 \times 10^{-4}$. Thus we get H_2 column density as a function of excess I(CII) for the above assumed $n(H_2)$ and T_K (see Langer at al. 2010b),

$$N(\mathrm{H_2})_{\mathrm{CII}} \sim 2.8 \times 10^{20} I(\mathrm{CII})_{\mathrm{H_2}}\ \mathrm{cm}^{-2}.$$

In Fig. 5 we show the distribution of the ratios of the H_2 column density traced by [CII] to that traced by ^{12}CO. In Table 2 we list a few diffuse clouds showing a large H_2 layer around the ^{12}CO emitting core. A majority of the clouds have $N(\mathrm{H_2})_{\mathrm{CII}} < N(\mathrm{H_2})_{^{12}\mathrm{CO}}$. In 15 clouds the $N(H_2)_{\mathrm{CII}}$ is 50% or greater than $N(\mathrm{H_2})_{^{12}\mathrm{CO}}$. In this sample of 50 transition clouds, on average, ~24% of the total H_2 column density is in the H_2/C^+ layer which is not traced by ^{12}CO. Although these estimates are only approximate, they show a likely scenario in the transition cloud structure. Lower densities (~100 cm^{-3}) and/or lower temperatures (~50 K) will increase the $N(H_2)$ in the H_2/C^+ layer (required to account for the observed I(CII)) by factors of 2–3, while higher density (~500 cm^{-3}) will decrease the $N(H_2)$ by a factor of 2. However, at higher densities the temperature is likely to be <100 K and the required $N(C^+)$ and $N(H_2)$ will be larger.

We can use $N(H_2)$ in the H_2/C^+ layer and N(HI) in the HI layer derived from I(CII) and I(HI) to evaluate A_V in the cloud up to the C^+/CO transition layer. We define the C^+/CO transition layer as an inner cloud boundary where $X(C^+) \sim X(\mathrm{CO}) = X(\mathrm{C_{total}})/2$. We can now solve for the ratio of external FUV to

Table 2. Selected transition cloud parameters.

Cloud	I(C II)	I(HI)	$I(^{12}CO)$	$N(H_2)$ in C^+	$N(H_2)$ in ^{12}CO	$[A_V\ (C^+/CO)]^1$	[FUV χ_0]^2	
Glong ± lat $V \pm V_{LSR}$	K km s^{-1}	K km s^{-1}	K km s^{-1}	10^{20}cm^{-2}	10^{20}cm^{-2}	mag	$\zeta_{standard}$	$40\zeta_{standard}$
G343.91+0.00V-14	6.2	647	1.6	9.6	2.9	1.65	1.11	9.26
G345.65+0.00V-19	3.2	238	1.6	6.0	3.0	0.88	0.07	0.84
G337.82+0.00V-127	6.1	330	10.8	12.9	19.5	1.70	1.07	9.14
G345.65+0.00V-120	6.7	263	6.4	15.2	11.5	1.89	1.91	15.5
G345.65+0.00V-114	3.9	182	3.6	8.5	6.5	1.09	0.15	1.61
G024.34+0.50V+116	5.1	279	6.7	10.1	12.1	1.43	0.46	4.31
G018.26-1.00V+58	2.3	271	1.96	3.1	3.5	0.59	0.02	0.33
G337.82+0.00V-118	8.2	414	11.6	17.2	20.9	1.80	1.38	11.60

Notes. [a] A_V corresponding to the C^+/CO layer. [2] External FUV radiation field derived for two cosmic ray ionization rates.

density ($\chi_0/n(H_2)$) balancing the photodissociation and the CO formation rates at the C^+/CO transition layer. We derive analytical photodissociation rates for the attenuation and the self-shielding which are consistent with those given by Lee et al. (1996). For simplicity in the warm regions (in all our chemical modeling and analysis we use $T_K \sim 100$ K) we consider only the H^+ + OI chemistry; however, detailed modeling should also include $C^+ + H_2$ radiative association. Therefore, for the CO formation rates we use a simple chemical network incorporating the H^+ + OI chemistry by extending the approach discussed by Nelson & Langer (1997) for a CO core surrounded by a warmer tenuous C^+ envelope. In our calculation we use the reaction rates given by Glover et al. (2010). The results for a few clouds are listed in Table 2; the last three columns list A_V up to the C^+/CO transition layer and the external FUV, χ_0, in units of Draine radiation field (χ_D). (Though the solution to the chemical modeling was obtained as $\chi_0/n(H_2)$ here we give only χ_0 as we have assumed $n(H_2)$= 300 cm^{-3} in our analysis of [CII] intensities). In nearly half of our sample the clouds have very low FUV, χ_0 in the range of 0.01 to 0.1χ_D. Such low values seem less likely in the ISM; it has been suggested that the [CII] in the ISM originates from clouds exposed to FUV, $\chi_0 > 10^{1.2}\chi_D$ (Cubick et al. 2008). Using PDR models (Pineda et al. 2010) find that in a [CII] sample of dense molecular clouds the majority have $\chi_0 = 1$–$10\chi_D$. Furthermore it may be noted that the H^+ + OI chemistry used here is sensitive to the cosmic ray (CR) ionization rate. Above we used the standard CR ionization rate $\zeta_{standard} \sim 2.5\times10^{-17}$ s^{-1}. However, there is recent evidence of much higher rates in the outer layers (low A_V) of clouds (Shaw et al. 2008; Indriolo et al. 2007, 2009). We find that using $40\zeta_{standard}$ increases the derived value of the FUV substantially as shown in the last column in Table 2. At least two of the clouds with high FUV values (G337.82+0.00V-127 and G337.82+0.00V-118) are near the supernova remnant G337.8-0.1, about a shell radius from its boundary at $V_{LSR} \sim -122$ km s^{-1} (Caswell et al. 1975), and thus may be consistent with our results for higher value for CR ionization. However, for the cloud G345.65+0.00V-120, though this LOS passes near a HII region (G345.645+0.010), no enhanced radiation feature is observed at this V_{LSR} (Caswell & Haynes 1987).

Our preliminary analysis assumes optically thin HI and C^+ emission. We do not take into account the different beam sizes used in the observations. We do not include the gas traced by CI in the C^+/CO transition zone. Nevertheless, the results of our simplified approach show a definite statistical trend for the presence of a majority of "nominal" diffuse clouds with a thin H_2 layer and a significant fraction of clouds with a thick H_2 layer without any accompanying CO.

4. Conclusions

We have observed [CII] line emission in 16 LOSs towards the inner Galaxy and detected 146 velocity resolved [CII] components. We identify 53 of these components that are characterized by the presence of both HI and ^{12}CO but no ^{13}CO emission as transition clouds in which the conversion of C^+ to CO is partial and a large fraction of carbon exists as C^+ mixed with H_2 in a "dark gas" layer surrounding the ^{12}CO emitting core. Our results show that [CII] emission is an excellent tool to study transition clouds in the ISM, in particular as a unique tracer of molecular H_2 which is not easily observed by other means. In about 10% of the clouds the H_2 column density traced by the [CII] emitting layer is greater than that traced by ^{12}CO emission. On average ~25% of the H_2 in these clouds is in the H_2/C^+ layer which is not traced by CO. Finally our estimates of the FUV field indicate the CR ionization is likely much larger than the standard value in the outer layers, consistent with recent determinations from chemical abundances in diffuse regions.

Acknowledgements. We thank the referee for suggestions. This work was performed by the Jet Propulsion Laboratory, California Institute of Technology, under contract with the National Aeronautics and Space Administration. The Mopra Telescope is managed by the Australia Telescope, and funded by the Commonwealth of Australia for operation as a National Facility by the CSIRO.

References

Abdo, A. A., Ackermann, M., Ajello, M., et al., 2010, ApJ, 710, 133
Caswell, J. L., & Haynes, R. F. 1987, A&A, 171, 261
Caswell, J. L., Murray, J. D., Roger, R. S., et al. 1975, A&A, 45, 239
Cubick, M., Stutzki, J., Ossenkopf, V., et al. 2008, A&A, 488, 623
Dame, T. M., Hartmann, D., & Thaddeus, P. 2001, ApJ, 547, 792
de Graauw, Th., Helmich, F. P., Phillips, T. G., et al. 2010, A&A, 518, L6
Draine, B. T. 1978, ApJS, 36, 595
Falgarone, E., Lis, D. C., Phillips, T. G., et al. 1994, ApJ, 436, 728
Glover, S. C. O., Federrath, C., Mac Low, M., et al. 2010, MNRAS, 404, 2
Goldsmith, P. F., Velusamy, T., Li, D., & Langer, W. D. 2010, ApJ, 715, 1370
Grenier, I. A., Casandjian, J.-M., & Terrier, R. 2005, Science, 307, 1292
Higgins, R. D., & Kooi, J. W. 2009, SPIE, 7215, 72150
Indriolo, N., Fields, B. D., & McCall, B. J. 2009, ApJ, 694, 257
Indriolo, N., Geballe, T. R., Oka, T., & McCall, B. J. 2007, ApJ, 671, 1736
Langer, W. D., Velusamy, T., Pineda, J. L., et al. 2010a, ESLAB2010, on line
Langer, W. D., Velusamy, T., Pineda, J. L., et al. 2010b, A&A, 521, L17
Nelson, R. P., & Langer, W. D. 1997, ApJ, 482, 796
Pilbratt, G. L., Riedinger, J. R., Passvogel, T., et al. 2010, A&A, 518, L1
Pineda, J. L., Velusamy, T., Langer, W. D., et al. 2010, A&A, 521, L19
Reach, W. T., Koo, B., & Heiles, C. 1994, ApJ, 429, 672
Shaw, G., Ferland, G. J., Srianand, R., et al. 2008, ApJ, 675, 405
Snow, T. P., & McCall, B. J. 2006, ARA&A, 44, 367
Stil, J. M., Taylor, A. R., Dickey, J. M., et al. 2006, AJ, 132, 1158
Tielens, A. G. G. M., & Hollenbach, D. 1985, ApJ, 291, 722
van Dishoeck, E. F., & Black, J. H. 1988, ApJ, 334, 771
Visser, R., van Dishoeck, E. F., & Black, J. H. 2009, A&A, 503, 323
Wolfire, M. G., Hollenbach, D., & McKee, C. F. 2010, ApJ, 716, 1191